Transient and quasistationary dissipative effects in the fission flux across the barrier in 1*A* GeV ^{238}U on deuterium reactions

J. Benlliure,[1,*] E. Casarejos,[1] J. Pereira,[1,†] and K.-H. Schmidt[2]
[1]*Universidad de Santiago de Compostela, E-15782 Santiago de Compostela, Spain*
[2]*Gesellschaft für Schwerionenforschung, D-64291 Darmstadt, Germany*
(Received 18 November 2005; revised manuscript received 6 March 2006; published 27 July 2006)

Isotopic cross sections of all projectile residues with Z above 23 produced in collisions induced by ^{238}U at 1A GeV on deuterium have been measured. The isotopic distributions reflect the role of evaporation and fission in the formation process of these nuclei. The comparison of the measured cross sections with Monte Carlo deexcitation codes including an analytical description of the dynamics of fission shows the sensitivity of the data to nuclear dissipation. Moreover, the large excitation-energy range covered in this experiment together with the high accuracy of the measured cross sections allowed to clearly separate and quantify the role of transient and quasistationary dissipative effects in the fission-decay width.

DOI: 10.1103/PhysRevC.74.014609 PACS number(s): 25.40.Sc, 25.85.Ge, 29.25.Rm

I. INTRODUCTION

Intense effort is being invested to improve our understanding of nuclear dynamics, e.g., the evolution of colliding nuclear systems and the fission process. Most successfully used theoretical approaches consider these processes in terms of a few macroscopic collective variables, representing the shape of the system, and the individual motion of noninteracting nucleons, describing the intrinsic excitation. The dynamics of the system is described by transport equations of the Fokker-Planck or the Langevin type in a nonequilibrium statistical approach. A fundamental nuclear property, appearing as a parameter in these models, is the viscosity, respectively, the dissipation strength, which measures the magnitude of the coupling between intrinsic and collective motion. This key property in particular governs the relaxation phenomena and diffusion processes of the nuclear system. Dissipation plays an essential role in the calculation of the formation cross sections of superheavy nuclei (e.g., Ref. [1]) and in a consistent description of the fission process (e.g., Ref. [2]). Still, the magnitude of the dissipation strength and in particular an eventual dependence on temperature and/or deformation is under debate. Different theoretical models (one-body dissipation [3], linear response [4]) yield diverging results. Moreover, quantum-mechanical effects, which go beyond these models, enter more and more into the discussion (e.g., Refs. [5–8]). In this situation, it is of prime importance to improve our empirical knowledge in this field by well adapted experimental approaches.

The fission process has probably been the most successful tool for investigating nuclear dissipation. It is characterized by a clearly observable large-scale collective motion, ending up in a binary decay of the system, which is in competition with statistical decay by sequential evaporation of nucleons and light clusters. Theoretically, one expects several phenomena to appear in fission due to nuclear viscosity: Firstly, the system might show relaxation effects while establishing the quasi-equilibrium distribution in the shape coordinates. This phenomenon was first studied by Grangé, Jung-Qing, and Weidenmüller [9] on the basis of the Fokker-Planck equation. As a consequence, the onset of the flow over the fission barrier is delayed by the transient time. The system may then cool down by evaporation, reducing the fission probability. Transient effects are expected to manifest only under specific experimental conditions [10]. Secondly, when quasiequilibrium is established, the quasistationary flow over the fission barrier is reduced with respect to the prediction of the Bohr-Wheeler transition-state model [11]. This reduction has already been deduced by Kramers [12], who derived an analytical solution of the Fokker-Planck equation for an inverted parabolic potential. These two phenomena, which influence the flow over the fission barrier, will be studied in the present work. Thirdly, another consequence of dissipation is an increase of the dynamical saddle-to-scission time in the quasistationary flow.

From the experimental side, there exist a number of observations that support the dynamical nature of the fission process. The anomalously enhanced prescission neutron multiplicities in fission induced in heavy-ion collisions [13,14] have been interpreted as a signature of the delay of fission at high excitation energies. Other evidences for dissipative effects were obtained from the analysis of gamma-rays emitted during the deexcitation of the GDR [15] or directly measuring the fission time using crystal blocking techniques [16,17]. From these experiments, the increase of the dynamical saddle-to-scission time due to dissipative effects appears to be a well-established phenomenon.

The experimental proof for dissipative effects on the flow over the fission barrier remains an important subject of intensive research. In contrast to heavy-ion fusion-fission reactions, which suffer from complex initial conditions, e.g., broad angular-momentum distributions and large shape distortions, nucleon-induced reactions or very peripheral nucleus-nucleus collisions at relativistic energies seem to be best suited for these studies.

*Electronic address: j.benlliure@usc.es
†Present address: NSCL, Michigan State University, East Lansing, Michigan 48824, USA.

Recently, a novel experimental approach has been introduced [18,19], which is based on the detection of fission products from nucleon-induced reactions or very peripheral nucleus-nucleus collisions at relativistic energies in inverse kinematics. The advantage of these reaction mechanisms is that the excited fissioning nucleus is produced with well-defined initial conditions. In particular, these reactions introduce only little shape distortions. In addition, they cover a large range in excitation energy while introducing only moderate angular momenta [21]. In these experiments, reaction residues with nearly projectile velocity are detected in forward direction. The inverse-kinematics conditions allow for identifying the fission products in atomic and mass number. These experiments were designed to be particularly sensitive to the time needed by the highly excited system to reach quasiequilibrium. In these works, the fission cross sections, the charge distribution [19], and the isotopic distribution [18] of fission residues have been used as signatures of the fission dynamics. Evidences for relaxation effects leading to transient times in the order of a few 10^{-21} s were deduced [18,19], which correspond to conditions close to the minimun possible transient time realized at critical damping [20].

For several years, also experiments on light charged-particle-induced reactions, e.g. Refs. [22,23] in conventional kinematics have been performed. In this case, evaporative neutrons and light charged particles were measured, from which initial thermal excitation energies were evaluated event by event. In addition, the fission fragments were registered, however, with a rather low resolution in mass. In a very recent letter [23], the measured fission probabilities of highly excited systems in 2.5-GeV proton-induced reactions were compared with model calculations. From this comparison the authors could not find any indication for dynamical effects on the flux over the fission barrier, since the data were fully explained by the statistical Bohr-Wheeler approach.

Thus, the findings deduced from the signatures of these two different experiments are in clear contradiction. In addition, the conclusions of Ref. [23] are rather intriguing by themselves. In particular, the following two statements of the paper are hardly compatible in view or our present theoretical understanding of the fission process: On the one hand, the protons are expected to induce only little collective excitations by angular momentum, shape distributions and compression. On the other hand, it is claimed that fission is in competition with particle evaporation immediately after the nuclear-collision stage of the reaction. It seems that the deduced immediate onset of fission requires a very fast population of the transition states above the fission barrier in a time well below the minimum transient time imaginable. Thus, the conclusions drawn in Ref. [23] seem to require a revised understanding of nuclear dynamics. If we admit that the inertia of the nuclear system is rather well established, it seems that the validity of the nonequilibrium statistical approach in terms of the transport equations of the Fokker-Planck or the Langevin type must be questioned.

The present work is intended to contribute to the solution of these problems. We investigate the reaction ^{238}U on deuterium at 1A GeV in inverse kinematics, taking advantage of the unique experimental installations of GSI. However, at this time we use a different observable, the isotopic production cross sections of evaporation residues. Due to the high fissility of the projectile, the yields of evaporation residues are expected to strongly depend on the fission process and in particular on transient and quasistationary dissipative effects on the fission flux across the barrier. In addition, the large excitation-energy range covered in the collisions induced by ^{238}U on deuterium can be sorted according to the mass loss of the final residues with respect to the projectile. Because of the narrow mass range produced in the collision stage of the reaction, the mass loss is dominated by the evaporation process, which is directly related to the excitation energy induced in the collision. One can then investigate the influence of transient and quasistationary dissipative effects in the fission flux as a function of the excitation energy involved in the fission process. Thus, the information on the physics of the fission process provided by the present experiment is very similar to the one obtained in Ref. [23], although it is based on different observables. In addition, the system is very similar, providing almost the same amount of center-of-mass energy.

II. EXPERIMENT AND RESULTS

The experiment was performed at GSI (Darmstadt) where the GSI Schwerionen Synchrotron (SIS) was used to produce a pulsed beam of ^{238}U at 1A GeV with a maximum intensity of 10^7 ions s^{-1}, a pulse length of 3 s and a repetition cycle of 7 s. This beam impinged onto a liquid-deuterium target with a thickness of 200 mg/cm^2. The cylindrical target container was 1 cm long and 3 cm in diameter with titanium windows of 18 mg/cm^2 in total.

Due to the inverse kinematics, the projectile residues produced in the reaction were emitted in forward direction and could be magnetically analysed in-flight with the fragment separator FRS [24]. This is an achromatic two-stage zero-degree spectrometer with a dispersive intermediate image plane. Every stage is equipped with two dipoles and a set of quadrupoles in front and behind each dipole. The resolving power of this device is $B\rho/\Delta B\rho \approx 1500$ with an acceptance of 15 mrad around the beam axis in angle and $\pm 1.5\%$ in momentum.

In order to isotopically identify all the transmitted nuclei, their horizontal positions at the intermediate and final image planes, their velocity and their energy loss in a given gas volume were measured with different detectors. Two plastic scintillators, about 20 cm long, 8 cm height and 5 mm thick, equipped with two photomultipliers at both extremes, were placed at the intermediate and final image planes to provide the position and time-of-flight measurements [25]. The atomic number of the nuclei was obtained from their energy-loss measurement in two multisampling ionisation chambers [26] located behind the spectrometer. Finally, a set of multiwire chambers placed at the different image planes of the spectrometer was used for calibration at the beginning of the experiment. In addition, and in order to identify the atomic number of heavy reaction residues with Z above 70, a velocity degrader [27] at the intermediate image plane of the spectrometer was used. The final resolution (FWHM) achieved for the mass and charge separation was

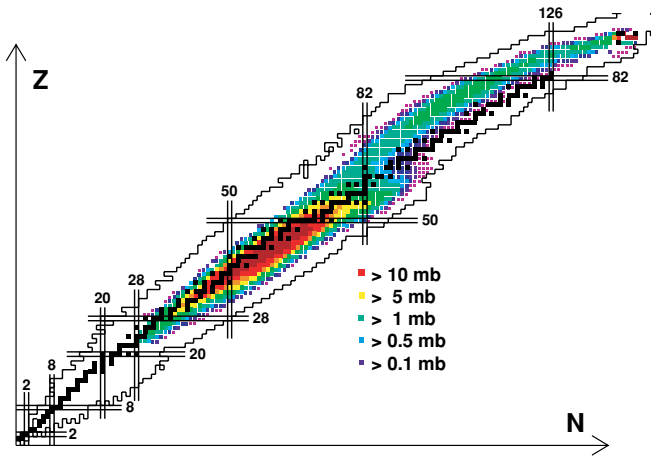

FIG. 1. (Color online) Two-dimensional cluster plot of all nuclei produced as projectile residues with a cross section larger than 100 μb in the reaction ^{238}U + ^{2}H at 1A GeV presented on top of the chart of the nuclides. The color scale represents the production cross section, the black squares correspond to stable isotopes, and the lines indicate the limit of the known nuclides.

$A/\Delta A \approx 400$ and $\Delta Z \approx 0.4$, respectively. The mass and charge identifications of the reaction residues were obtained by using the primary beam as reference and the specific pattern of light nuclei when represented on a two-dimensional spectrum A/Z versus Z [28].

Due to the limited acceptance of the spectrometer, more than 50 different magnetic tunings of the dipoles of the FRS were needed to completely measure the momentum distributions of all nuclear species produced in the reaction ^{238}U on deuterium at 1A GeV with a production cross section above 100 μb and $Z > 23$. Using the information provided by the beam-monitor detector SEETRAM [29], the yields measured in different magnetic tunings were normalized and combined to produce the corresponding momentum distribution for each nuclide. The integral of these momentum distributions normalized to the number of atoms in the target and corrected for the detection efficiency, angular transmission and secondary reactions provided the production cross sections of all measured nuclei. A detailed description of the experiment and the data analysis can be found in Refs. [30–33].

The results of the experiment are summarised in Fig. 1. In this figure, we represent in a two-dimensional cluster plot all the projectile residues produced in the reaction ^{238}U with deuterons at 1A GeV, with a cross section larger than 100 μb and Z above 23, on top of a chart of the nuclides. More than 1400 different nuclides have been identified, and their cross sections have been determined with an accuracy between 10% and 20%. In the figure we can clearly observe two different groups of nuclides. The upper part of the chart of the nuclides is populated by mostly neutron-deficient nuclides covering a large range in charge from the projectile nucleus down to the charge 65. On average, for a given element, the isotopic distribution covers around 20 different nuclides with a maximum production cross section around a few millibarns. These nuclei are produced in a nucleon and/or cluster evaporation process from the excited projectile prefragments produced in the interaction between the projectile and the target nuclei. This process leads to residual nuclei lighter than the projectile with an isotopic composition determined by the competition between neutron and proton evaporation and the initial excitation energy induced in the collision. Since the evaporation of protons and neutrons is governed not only by the respective binding energies but also by the proton Coulomb barrier, the equilibrium between both processes is reached at the left of the stability line, along the so called "evaporation corridor" [34], defining the ridge line of the nuclide distributions of evaporation residues. The initial excitation energy determines the length of the evaporation chain and consequently the mass of the final residue. Since the number of nucleons removed from the projectile in direct collisions with the target deuteron is expected to be rather small, the mass of the evaporation residues is an observable which is well correlated with the excitation energy induced in the reaction. This important aspect will be discussed later in further detail.

The second group of nuclei observed in Fig. 1 corresponds to medium-mass fragments with atomic numbers between 23 and 65. In this case, the isotopic distributions are broader, populating on average 25 isotopes. The distributions are centred to the right of the stability line, and the production cross sections are much larger than the ones observed for the evaporation residues. These nuclei are expected to be produced by fission of the projectile prefragments emerging from the interaction between the ^{238}U projectiles with deuterium. The fission process preserves the neutron excess of the fissioning nucleus, in our case the projectile prefragment, at low excitation energy. However, when the system crosses the fission saddle at high excitation energies, this neutron excess is partially lost by neutron evaporation, both from the system on the way to scission and from the fragments, shifting and broadening the final isotopic distribution of the fission residues. The observed mass distribution of fission residues is mostly single-humped, in contrast to the well known double-humped distribution of residues produced in the low-energy fission of ^{238}U, indicating in our case that fission takes place at high excitation energy, where shell effects are washed out. Nevertheless, the most neutron-rich fission residues show a contribution by a double-humped component resulting from low-energy fission induced in very peripheral reactions.

From the analysis of Fig. 1 we can conclude that fission is the dominant deexcitation channel in the reaction ^{238}U on deuterium at 1A GeV. A similar conclusion can be drawn from Fig. 2(a). In this figure, we represent the isobaric distribution of projectile residues as a function of their mass loss (ΔA) with respect to the mass of the projectile, measured in the reaction ^{238}U(1A GeV) on deuterium (black dots) compared to the one obtained for the reaction ^{208}Pb(1A GeV) on deuterium (grey/red dots) [35]. We can also identify in both cases the two groups of residues produced in evaporation and fission processes, respectively. Although the excitation energy induced in both reactions should be similar, fission seems to be the dominant reaction channel in the collisions induced by ^{238}U, while in the case of the reactions induced by ^{208}Pb we arrive at the opposite conclusion. This result can

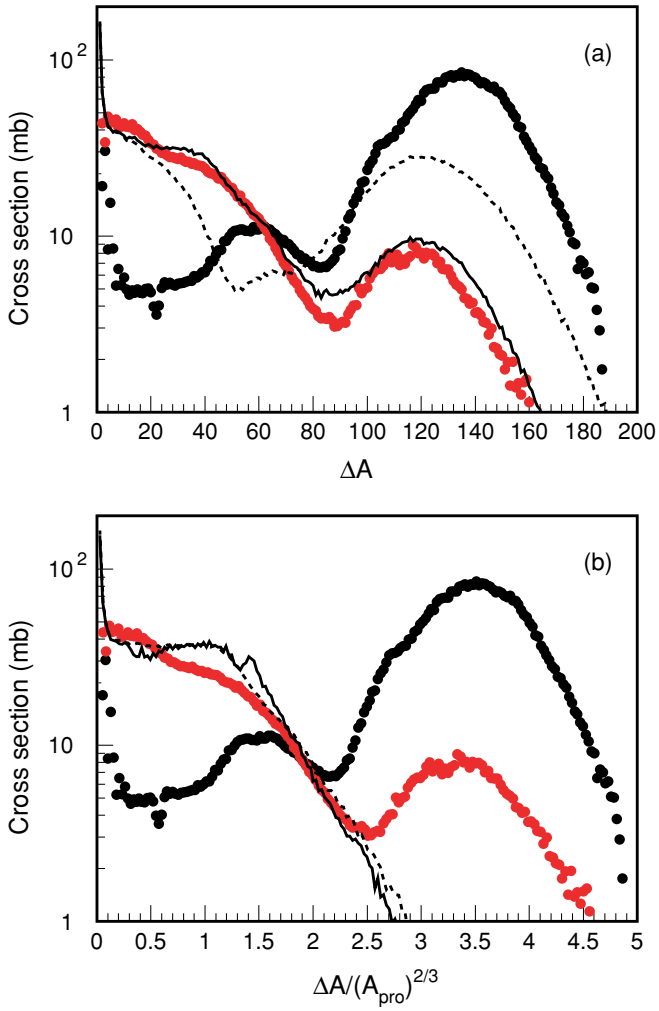

FIG. 2. (Color online) Isobaric distributions of projectile residues produced in reactions induced by ^{238}U(1A GeV) (black dots) and ^{208}Pb(1A GeV) (grey/red dots) [35] on deuterium as a function of the mass loss of the final residues (ΔA) with respect to the projectile. In the bottom panel, the mass loss of the final residue is normalized to the initial mass number of the projectile to the power of 2/3. In (a) the isobaric distribution of residues produced in the reaction ^{208}Pb(1A GeV) on deuterium is compared to model calculations performed with the Isabel intranuclear cascade code [36] coupled to the ABLA evaporation code [37,40] with a dynamical description of fission according to Ref. [10] (solid line) and a purely statistical description of fission (dashed line). In (b) both sets of data are compared to calculations where fission has been suppressed (solid line ^{238}U(1A GeV) + ^{2}H and dashed line ^{208}Pb(1A GeV) + ^{2}H).

be attributed to the different fissilities of the prefragments produced in both reactions. Since the fission component for the ^{208}Pb system represents less than 15% of the total cross section, and the total cross sections for the reactions ^{238}U(1A GeV) and ^{208}Pb(1A GeV) on deuterium differ by less than 15%, we can conclude that the differences observed in Fig. 2(a) for the isobaric distributions of evaporation residues in both reactions are due to the stronger influence of fission in the reactions induced by ^{238}U at 1A GeV on deuterium.

III. ANALYSIS OF DISSIPATIVE EFFECTS

A. Model description

A deeper and more quantitative interpretation of our data requires the use of model calculations. In order to describe the interaction of deuterons with ^{238}U and ^{208}Pb at relativistic energies, we used an intranuclear cascade code coupled to a deexcitation code considering both nucleon and/or cluster evaporation and fission. After benchmarking different intranuclear-cascade models, the most consistent description of the available data on ^{238}U + ^{2}H and ^{208}Pb + ^{2}H [35], which are characterised by substantially different fissilities, was obtained with the Isabel code of Yariv and Fraenkel [36]. The evaporation and fission processes were described using the Monte Carlo code ABLA. In this code the evaporation of nucleons and alpha clusters is described according to the Weisskopf formalism including a consistent description of level densities where shell, pairing and collective effects are considered following reference [37]. The fission width is calculated using the statistical approach of Bohr and Wheeler $\Gamma_{\rm BW}$ [11], corrected for quasi-stationary and transient dissipative effects, which describe the dynamical nature of fission according to

$$\Gamma_f(t) = \Gamma_{\rm BW} \cdot K \cdot f(t). \tag{1}$$

In this equation K represents the so-called Kramers coefficient which provides the correction one has to apply to the statistical fission width in order to obtain the quasistationary solution of the Fokker-Plack equation describing the fission flux across the barrier [12]. This factor is defined as

$$K = \left\{ \left[1 + \left(\frac{\beta}{2\omega_o} \right)^2 \right]^{1/2} - \frac{\beta}{2\omega_o} \right\}, \tag{2}$$

where β is the reduced dissipation coefficient, and ω_o corresponds to the frequency of the harmonic oscillator describing the inverted potential at the fission barrier.

In Eq. (1), the function $f(t)$ describes the time dependence of the fission width resulting from the time-dependent solution of the Fokker-Planck equation used by Grangé, Jun-Qing, and Weidenmüller [9]. The analytical approach of Ref. [10] to Eq. (1) makes it possible to avoid the computational effort required to solve numerically the Fokker-Planck equation on an event-by-event basis. In our Monte Carlo code we can also use other analytical approximations to describe the time dependence of the fission width $f(t)$ that will be discussed in the next section.

The main consequence of Eq. (2) is that the quasistationary and transient effects that appear in the dynamical description of the fission flux across the barrier lead to a reduction of the fission width compared to the value obtained with the statistical model.

Besides nuclear dissipation, the fission barriers and even more the level densities are the ingredients of the model description, which have the most important influence on the fission probabilities at high excitation energies and thus should be considered with special care. In addition to the arguments given in Ref. [18], which already justified the choice of Refs. [38] and [39] for the description of fission

barriers and level densities, the deformation dependence of the level-density parameter, which is the basis for their ratio at the transition-state and ground-state deformation a_f/a_n used in our calculation, has been investigated recently on the basis of the Yukawa-plus-exponential description of the nuclear properties [41,42]. Also this theoretical study has essentially confirmed the validity of Ref. [39], which we use in our calculation.

Finally, the isotopic distribution of fission residues is described following the model of reference [40]. In addition, the ABLA code includes a breakup channel which sets in when the nuclear temperatures reaches 5 MeV [43].

An example of the results obtained with this model is shown in Fig. 2 for the reaction ^{208}Pb(1A GeV) on deuterium. The solid line in Fig. 2(a) corresponds to a calculation where we describe the fission dynamics by means of the analytical approximate solution of the time-dependent Fokker-Planck equation, proposed by Jurado and collaborators [10,20] (see next section), with a reduced dissipation coefficient $\beta = 2 \times 10^{21} s^{-1}$. In this panel, the data are also compared to a calculation using a purely statistical description of the fission width (dashed line) that clearly overestimates the fission probability.

This reaction can be considered as an optimum case to benchmark the intra-nuclear and the evaporation code, since in this case the role of fission is minor as shown by the dashed line in Fig. 2(b), representing a calculation for the reaction ^{208}Pb(1A GeV) on deuterium where fission has been completely suppressed. Moreover, in this reaction the description of the level densities is simpler since only few nuclei will feel the $Z = 82$ shell, and the collective enhancement for the deformed nuclei is expected to be almost the same for the different deexcitation channels, e.g., in the ground state for particle emission and at the saddle for fission. The minor role of fission and the good description of the production cross sections provided by the dynamical calculation for both, evaporation and fission residues, validate the intranuclear cascade model as well as the description of the evaporation channels and the breakup, which plays a role only for the lightest evaporation residues.

B. Discussion

In order to better understand the general trends of the reaction ^{238}U(1A GeV) + ^{2}H, we show in Fig. 3 the calculated excitation energy of the initial prefragments as a function of the mass loss of the final residue (ΔA) with respect to the projectile. This calculation was done with the same description of the fission width represented by the solid line in Fig. 2(a).

As can be seen, only evaporation residues ($\Delta A < 90$) exhibit a clear correlation between their final masses and the initial excitation energies of the decaying prefragments. Applying different intranuclear cascade codes [36,44], we found that this correlation is a common feature, which quantitatively varies only little for the different codes. We understand this result as a consequence of a rather strict correlation between the initial excitation energy and the mass loss in the deexcitation stage, the mass loss in the intranuclear cascade stage being

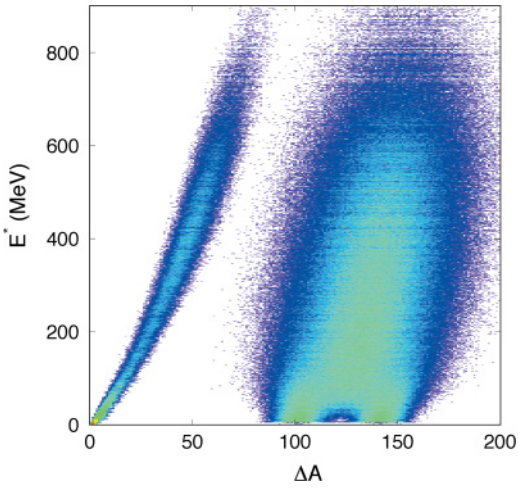

FIG. 3. (Color online) Excitation energy of the initial prefragments as a function of the mass loss of the final residue with respect to the projectile for the reaction ^{238}U (1A GeV) + ^{2}H.

comparably small. Indeed, Fig. 3 provides an energy scale to the abscissa of Fig. 2(a) for the ^{238}U(1A GeV) + ^{2}H reaction.

In order to compare both reactions, ^{238}U(1A GeV) and ^{208}Pb(1A GeV) on deuterium, with the same scale of initial excitation energy, in the bottom panel of Fig. 2 we have normalized the abcissa ΔA to the initial mass number of the projectile to the power 2/3, $(A_{\rm pro})^{2/3}$. This factor provided the best normalization to account for size effects in the amount of the deposited excitation energy in both reactions. In this figure we also compare the data with calculations where fission has been suppressed [solid line for ^{238}U(1A GeV) + ^{2}H and dashed line for ^{208}Pb(1A GeV) + ^{2}H]. As can be seen, both calculations almost coincide [the slight differences observed for the light evaporation residues could be due to the fact that the initial excitation energy does not scale exactly with $(A_{\rm pro})^{2/3}$], fairly describe the production of evaporation residues in reactions induced by ^{208}Pb at 1A GeV and largely overestimate the production of evaporation residues for the reaction ^{238}U(1A GeV) + ^{2}H for mass losses up to 50 units ($\Delta A/(A_{\rm pro})^{2/3} \approx 1.3$). This result clearly indicates that the fission channel dominates the deexcitation process of prefragments produced in the reaction ^{238}U(1A GeV) on deuterium at low and moderate excitation energies. Moreover, the coincidence between both calculations and the fact that they reproduce the measured data for both reactions around $\Delta A = 65$ ($\Delta A/(A_{\rm pro})^{2/3} \approx 1.8$) also indicates that fission plays a minor role in the de-excitation of highly excited prefragments (large mass losses). This is a surprising result that clearly contradicts the expectations due to the statistical description of the fission process according to the model of Bohr and Wheeler [11] (dotted line in Fig. 4). This inhibition of fission at high excitation energies would qualitatively fit with the dynamical interpretation of fission as proposed by Kramers [12] and later on by Grangé, Jun-Qing and Weidenmüller [9].

Once we have validated most of the ingredients in our code we can concentrate on the fission channel which is the dominant one in the reaction induced by ^{238}U. In Fig. 4, we compare the measured isobaric distribution of projectile

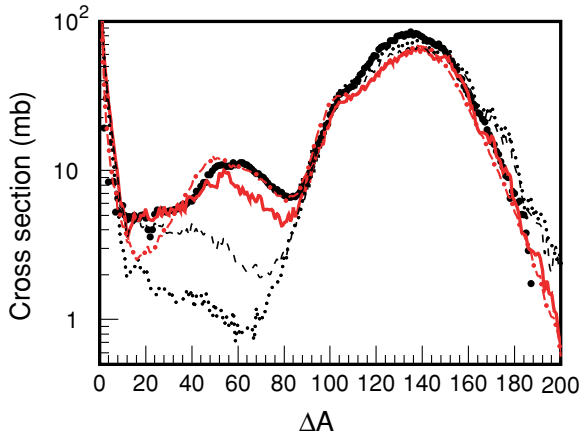

FIG. 4. (Color online) Measured isobaric distribution of evaporation residues produced in the reaction ^{238}U(1A GeV) + ^{2}H (dots), compared with different calculations performed with the Isabel intranuclear cascade code coupled to the ABLA evaporation code. The dotted line represents a calculation using a purely statistical description of fission and deformation-dependent level-density parameters. The calculation represented by the dashed line includes the Kramers factor in the fission width with $\beta = 2 \times 10^{21}$ s^{-1} and the solid line represents a calculation with not only the Kramers factor but also the time dependence of the fission width. Both calculations use deformation-dependent level-density parameters. Finally, the dashed-dotted line corresponds to a calculation using a purely statistical description of fission with no deformation-dependent level-density parameters ($a_f/a_n = 1$).

residues produced in the reaction ^{238}U(1A GeV) + ^{2}H (dots) with different model calculations. All these calculations, including different descriptions of the fission dynamics at high excitation energy, provide a quite similar description of the fission residues. This result can be understood considering that an important fraction of the fission probability concentrates at relatively low excitation enegy ($E < 200$ MeV, see Fig. 3) where these calculations have a similar description of the fission probability. Moreover, in the case of fission the mass loss of the final residues with respect to the projectile does not constitute a good excitation-energy filter as shown in Fig. 3. The sensitivity to the different descriptions of the fission dynamics at high excitation energy appears in the evaporation residues since they represent the survival probablility against fission and their mass loss presents a good correlation with the excitation energy.

The dotted line in Fig. 4 was obtained using the purely statistical model of Bohr and Wheeler [11]. As can be seen, this model clearly overestimates the fission channel at high excitation energy depopulating the production of evaporation residues. Better agreement with the measured data is obtained when the dynamics of fission is considered in the calculation. The dashed line corresponds to a calculation where the fission width is evaluated using the Kramers factor described by Eq. (2) with a reduced viscosity parameter of $\beta = 2 \times 10^{21}$ s^{-1}. However, a calculation considering not only the quasistationary effects in the fission flux by means of the Kramers factor with $\beta = 2 \times 10^{21}$ s^{-1}, but also the transient effects due to the time dependence of the fission width (solid line) provides the best description of the data. In this case, the time dependence of the fission width has been calculated according to the approximate solution of the Fokker-Planck equation proposed by Jurado and collaborators [10,20].

The fair agreement observed in Fig. 4 between our calculations (solid line) and the experimental data (dots) is consistent with previous investigations where different observables and reactions have been used. In particular, partial fission cross sections and final charge distributions of fission residues produced in the reaction ^{238}U(1A GeV) + CH_2 [19], total fission cross section and the isotopic distribution of fission residues in collisions induced by ^{197}Au on hydrogen at 800A MeV [18] and the present isotopic distributions of evaporation residues produced in the reaction ^{238}U at 1A GeV on deuterium, are coherently reproduced by these calculations.

However, until now, none of the observables used as signatures of the fission dynamics allowed us to characterise and quantify independently the role of transient and quasistationary dissipative effects in the fission flux at small deformation. In principle one would expect low-energy fission to be sensitive to quasistationary effects, characterized by the reduced dissipation coefficient in Kramers factor, and not to transient effects, which are expected to be much shorter than the statistical fission time at low excitation energy. On the other hand, as the excitation energy increases, the statistical fission time approaches the transient time, and the fission process becomes sensitive to this latter effect. The strong correlation between the final mass of the evaporation residues and the initial excitation energy, together with the large excitation-energy range covered with the reaction ^{238}U at 1A GeV on deuterium allowed us to analyse our data following these ideas.

In Fig. 5 we show the isobaric distribution of evaporation residues produced in the reaction ^{238}U at 1A GeV on deuterium compared with calculations using different reduced dissipation coefficients and descriptions of the time-dependent fission width. In the left panel of the figure we compare the measured data to calculations, where different values of the reduced dissipation coefficient β have been used, $\beta = 1 \times 10^{21}$ s^{-1}(dashed line), $\beta = 2 \times 10^{21}$ s^{-1}(solid line), $\beta = 3 \times 10^{21}$ s^{-1} (dotted line) and $\beta = 5 \times 10^{21}$ s^{-1} (dashed-dotted line). In all these calculations the time dependence of the fission width has been described using the approximate solution of the Fokker-Planck equation proposed by Jurado *et al.* [10,20]. These calculations clearly show how the measured yields of evaporation residues depend on the value of the reduced dissipation coefficient. Even more, this effect manifests mainly in heavy evaporation residues corresponding to the survival probability against fission at low or moderate excitation energies. As already stated, the value of the reduced dissipation coefficient $\beta = 2 \times 10^{21}$ s^{-1} reproduces the data fairly well.

In the right panel of Fig. 5, we compare the same data to another set of model calculations. At this time we have fixed the value of the reduced dissipation coefficient to $\beta = 2 \times 10^{21}$ s^{-1}, and we have used different models to describe the time dependence of the fission width. The result of the calculation using the approximate solution of the Fokker-Planck equation proposed by Jurado *et al.* [10,20] is represented

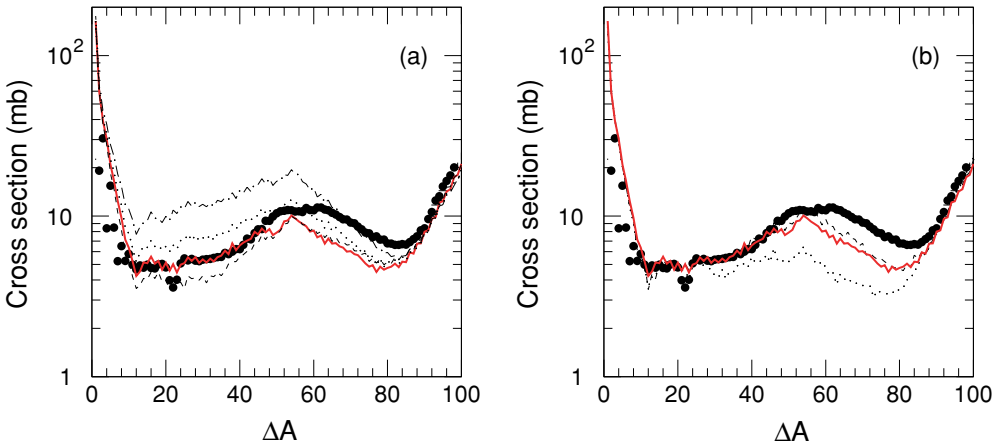

FIG. 5. (Color online) Isobaric distribution of evaporation residues produced in the reaction $^{238}U + ^{2}H$ at 1A GeV (dots). In the left panel, the data are compared to calculations using different values of β: 1×10^{21} s^{-1} (dashed line), 2×10^{21} s^{-1} (solid line), 3×10^{21} s^{-1} (dotted line) and 5×10^{21} s^{-1} (dashed-dotted line), in all these calculations the time dependence of the fission width follows the analytical solution of the Fokker-Planck equation. In the right panel, we compare calculations with $\beta = 2 \times 10^{21}$ s^{-1}, but different time dependences of the fission width: an exponential in-growth function (dotted line), a step function (dashed line) and the analytical solution of the Fokker-Planck equation (solid line).

by the solid line. According to this approximation the time dependence of the fission width can we expressed as

$$\Gamma_f(t) \approx K \cdot \Gamma_{\mathrm{BW}} \cdot \frac{W_n(x = x_b; t, \beta)}{W_n(x = x_b; t \to \infty, \beta)}, \tag{3}$$

where K is the Kramers factor, Γ_{BW} the statistical fission width and $W_n(x = x_b; t, \beta)$ the normalized probability distribution at the barrier deformation x_b. In this expression we neglect the variation of the mean velocity of the fission trajectories at saddle with time [20]. Moreover, we approximate the probability distribution at saddle by the solution of the Fokker-Planck equation for a parabolic potential [45], which has been derived for the very specific initial condition of a delta function at zero deformation and zero velocity for $t = 0$:

$$W_n(x = x_b; t, \beta) = \frac{1}{\sqrt{2\pi}\sigma} \exp\left(-\frac{x_b^2}{2\sigma^2}\right), \tag{4}$$

where σ^2 is a time-dependent function of the form

$$\sigma^2 = \frac{T}{\mu\omega_1^2}\left\{1 - \exp(-\beta t)\left[\frac{2\beta^2}{\beta_1^2}\sinh^2\left(\frac{\beta_1 t}{2}\right) + \frac{\beta}{\beta_1}\sinh(\beta_1 t) + 1\right]\right\} \tag{5}$$

being T the nuclear temperature, μ the reduced mass associated to the deformation degree of freedom, ω_1 the curvature of the potential at the ground state and $\beta_1 = (\beta^2 - 4\omega_1^2)^{1/2}$. A more realistic description should consider an initial distribution $W_n(x, t, \beta)$ with a minimum width due to quantum-mechanical effects or even the intital shape distortion introduced by the reaction. In our case we just considered the quantum-mechanical effects by a shifted time scale ($t' = t + t_{zp}$) in Eqs. (4) and (5) where t_{zp} was chosen such that $W_n(x, t', \beta)$ for $t = 0$ corresponds to the distribution defined by the zero-point motion of the projectile around a spherical shape [46]. Implementing Eqs. (4) and (5), including the time shift, in Eq. (3) we obtain an analytical expression for $\Gamma_f(t)$.

The dotted line in Fig. 5(a) corresponds to an exponential in-growth time dependence of the fission width [47]

$$\Gamma_f(t) = K \cdot \Gamma_{\mathrm{BW}} \cdot \{1 - \exp(-t/\tau)\}, \tag{6}$$

where $\tau = \tau_{\mathrm{trans}}/2.3$ with τ_{trans} being the transient time defined as the time the fissioning system needs to reach 90% of the stationary fission-decay width across the barrier. In this figure, the dashed line represents the result obtained with a time dependence of the fission width following a step function [48]:

$$\Gamma_f(t) = \begin{cases} 0 & t < \tau_{\mathrm{trans}} \\ K \cdot \Gamma_{\mathrm{BW}} & t \geqslant \tau_{\mathrm{trans}}. \end{cases} \tag{7}$$

From this comparison we can conclude that the time dependence of the fission width based on the approximate solution of the Fokker-Planck equation and the step function provide similar results, although the first one has a better physical justification. The exponential in-growth clearly overestimates the fission width, in particular at high excitation energies (short times) as was already pointed out in Ref. [20]. In addition, we can also conclude that in contrast to the calculations performed with different values of the reduced dissipation coefficient β, in this case the sensitivity of the data to the transient effects appears for large values of the mass loss of the residues corresponding to high excitation energies. Consequently, our data make it possible to decouple the role of transient and quasi-stationary dissipative effects in the fission flux. We describe the evaporation-residue cross sections for a large mass range with the same value of the reduced dissipation coefficient ($\beta = 2 \times 10^{21}$ s^{-1}) fairly well. Slight deviations for the lightest residues might indicate an even stronger suppression of fission at the highest excitation energies, since the measured cross sections of these residues are slightly underestimated by the calculation. Before drawing more quantitative conclusions, improved theoretical calculations are

planned to better describe the entrance-channel distribution of the prefragments in deformation space, which we assumed to be identical to the zero-point motion of the projectile around a spherical shape in the present analysis.

When we compare our conclusions with the ones drawn in Ref. [23], we observe a severe discrepancy. While we find strong indications for dissipative effects in the magnitude of the evaporation-residue cross sections, the essentially complementary fission probabilities measured in Ref. [23] were fully reproduced by calculations with the purely statistical Bohr-Wheeler approach. For the system $^{238}\mathrm{U}+^{2}\mathrm{H}$, we noticed an essential difference in the ingredients of the model calculation, which probably explains the controversial conclusions: While we determine the appropriate value of a_f/a_n according to the saddle-point deformation of each fissioning system following the description of Ignatyuk *et al.* [39] for the deformation dependence of the level density parameter, Tishchenko *et al.* [23] use a common value of $a_f/a_n = 1$ for all fissioning systems produced in the collision of ^{238}U with 2.5 GeV protons, which extend over a broad range of elements [19]. With the option $a_f/a_n = 1$, we can also reproduce our data (dashed-dotted line in Fig. 4) and the fission probabilities reported in Ref. [23] within the Bohr-Wheeler statistical approach fairly well without introducing any transient effects. However, as already mentioned, this option is not compatible with the conclusions of Refs. [39,42]. Thus, the diverging findings of Tishschenko *et al.* and the present work for the fission of ^{238}U by 2 GeV light charged particles seem to be traced back to different ingredients of the model calculations.

A discussion of the results for the lighter systems also studied in Ref. [23] is beyond the scope of the present work. We will address this interesting subject in the near future, when data from inverse-kinematics experiments for similar systems will be available.

IV. CONCLUSION

In this work, we have shown that the accurate measurement of the isotopic production of reaction residues provides valuable information on the reaction mechanism. In particular, we have presented the measured isotopic cross sections of more than 1400 different projectile residues produced in the reaction ^{238}U(1A GeV) on deuterium with an accuracy between 10% and 20%. In this reaction, the dominant fission channel can be investigated from the measured fission residues or from the survival probability against fission, represented by the evaporation residues. The strong correlation existing between the mass loss of the evaporation residues and the initial excitation energy induced in the collisions offers the possibility to use these residual nuclei for investigating the excitation-energy dependence of the fission process. The comparison of these data with the evaporation residues produced in the reaction ^{208}Pb(1A GeV) on deuterium clearly shows the dominance of fission in the ^{238}U-induced reaction. However, the fact that for large mass losses both reactions lead to the production of residues with similar cross sections represents a clear signature of the suppression of fission in the ^{238}U-induced reactions at high excitation energies. Model calculations show that the measured data can only be understood when the dynamics of fission is considered, in agreement with previous works. Moreover, the accuracy of the present data, together with the large excitation-energy range covered with this reaction made it possible to characterise and quantify independently the role of transient and quasistationary dissipative effects in the fission flux across the barrier. The cross sections in the whole mass range are fairly well reproduced with a single value of the dissipation coefficient $\beta = 2 \times 10^{21}$ s^{-1}. The same calculations and parameters also describe the ^{208}Pb-induced reactions and other data investigated in previous works [10,18].

Discrepancies in the interpretation of similar data recently obtained by Tishchenko *et al.* [23] in direct kinematics were understood in terms of the different ingredients used in the model calculations. The use of appropriate values for the level-density parameter and in particular its dependence on deformation appears to be crucial for the correct understanding of the fission dynamics at high excitation energy.

ACKNOWLEDGMENTS

We thank B. Jurado, A. Kelic, F. Rejmund, and C. Volant for valuable discussions as well as T. Enqvist for the careful reading of the manuscript. This work was partially supported by the European Commission through the HINDAS project under contract FIKW-CT-2000-031 and the Spanish MEC and XuGa under contracts FPA2002-04181-C04-01 and PGIDT01PXI20603PM, respectively.

[1] Y. Abe, Eur. Phys. J. A **13**, 143 (2002).
[2] P. N. Nadtochy, G. D. Adeev, and A. V. Karpov, Phys. Rev. C **65**, 064615 (2002).
[3] J. Randrup and W. J. Swiatecki, Ann. Phys. (NY) **125**, 193 (1980).
[4] H. Hofmann, Phys. Rep. **284**, 137 (1997).
[5] G. Abal, Romanelli, A. C. Sicardi-Schifino, R. Siri, and R. Donangelo, Nucl. Phys. **A683**, 279 (2001).
[6] L. Capriotti, A. Cuccoli, A. Fubini, V. Tognetti, and R. Vaia, Europhys. Lett. **58**, 155 (2002).
[7] N. Takigawa, S. Ayik, K. Washiyama, and S. Kimura, Phys. Rev. C **69**, 054605 (2004).
[8] S. Radionov and S. Aberg, Phys. Rev. C **71**, 064304 (2005).
[9] P. Grangé, LiJun-Qing, and H. A. Weidenmüller, Phys. Rev. C **27**, 2063 (1983).
[10] B. Jurado *et al.*, Nucl. Phys. **A757**, 329 (2005).
[11] N. Bohr and J. A. Wheeler, Phys. Rev. **56**, 426 (1939).
[12] H. A. Kramers, Physika VII **4**, 284 (1940).
[13] A. Gavron *et al.*, Phys. Rev. Lett. **47**, 1255 (1981).
[14] D. J. Hilscher and H. Rossner, Ann. Phys. Fr. **17**, 471 (1992).

[15] P. Paul and M. Thönnessen, Annu. Rev. Nucl. Part. Sci. **44**, 65 (1994).
[16] W. M. Gibson, Annu. Rev. Nucl. Sci. **25**, 465 (1975).
[17] I. Gontchar, M. Morjean, and S. Basnary, Europhys. Lett. **57**, 355 (2002).
[18] J. Benlliure *et al*., Nucl. Phys. **A700**, 469 (2002).
[19] B. Jurado, C. Schmitt, K. H. Schmidt, J. Benlliure, T. Enqvist, A. R. Junghans, A. Kelic, and F. Rejmund, Phys. Rev. Lett. **93**, 072501 (2004).
[20] B. Jurado *et al*., Nucl. Phys. **A747**, 14 (2005).
[21] M. de Jong, A. V. Ignatyuk, and K.-H. Schmidt, Nucl. Phys. **A613**, 435 (1997).
[22] S. Schmid *et al*., Z. Phys. A **359**, 27 (1997).
[23] V. Tishchenko, C. M. Herbach, D. Hilscher, U. Jahnke, J. Galin, F. Goldenbaum, A. Letourneau, and W. U. Schroder, Phys. Rev. Lett. **95**, 162701 (2005).
[24] H. Geissel *et al*., Nucl. Instrum. Methods B **70**, 286 (1992).
[25] B. Voss *et al*., Nucl. Instrum. Methods A **364**, 150 (1995).
[26] M. Pfützner *et al*., Nucl. Instrum. Methods B **86**, 213 (1994).
[27] K.-H. Schmidt *et al*., Nucl. Instrum. Methods A **260**, 287 (1987).
[28] M. V. Ricciardi *et al*., Phys. Rev. C **73**, 014607 (2006).
[29] A. R. Junghans *et al*., Nucl. Instrum. Methods A **370**, 312 (1996).
[30] E. Casarejos *et al*., accepted for publication by Phys. Rev. C.
[31] J. Pereira *et al*., submitted to Phys. Rev. C.
[32] J. Taieb *et al*., Nucl. Phys. **A724**, 413 (2003).
[33] M. Bernas *et al*., Nucl. Phys. **A725**, 213 (2003).
[34] J. P. Dufour *et al*., Nucl. Phys. **A387**, 157c (1982).
[35] T. Enqvist *et al*., Nucl. Phys. **A703**, 435 (2002).
[36] Y. Yariv and Z. Fraenkel, Phys. Rev. C **24**, 488 (1981).
[37] A. R. Junghans *et al*., Nucl. Phys. **A629**, 635 (1998).
[38] A. J. Sierk, Phys. Rev. C **33**, 2039 (1986).
[39] A. V. Ignatyuk, M. G. Itkis, V. N. Okolovich, G. N. Smirekin, and A. S. Tishin, Yad. Fiz. **21**, 1185 (1975); Sov. J. Nucl. Phys. **21**, 612 (1975).
[40] J. Benlliure *et al*., Nucl. Phys. **A628**, 458 (1998).
[41] H. J. Krappe, Phys. Rev. C **59**, 2640 (1999).
[42] A. V. Karpov, P. N. Nadtochy, E. G. Ryabov, and G. D. Adeev, J. Phys. G **29**, 2365 (2003).
[43] K.-H. Schmidt *et al*., Nucl. Phys. **A710**, 157 (2002).
[44] A. Boudard, J. Cugnon, S. Leray, and C. Volant, Phys. Rev. C **66**, 044615 (2002).
[45] S. Chandrasekhar, Rev. Mod. Phys. **15**, 1 (1943).
[46] B. Jurado, K.-H. Schmidt, and J. Benlliure, Phys. Lett. **B533**, 186 (2003).
[47] R. Butsch, D. J. Hofman, C. P. Montoya, P. Paul, and M. Thoennessen, Phys. Rev. C **44**, 1515 (1991).
[48] E. M. Rastopchin *et al*., Yad. Fiz. **53**, 1200 (1991) [Sov. J. Nucl. Phys. **53**, 741 (1991).]